

# Study of $\text{Na}_2\text{O}-\text{SiO}_2-\text{Fe}_2\text{O}_3-\text{Y}_2\text{O}_3$ glass by Mössbauer and EPR spectroscopy

AKHILESH PRASAD, D. BAHADUR\*, R. M. SINGRU,  
D. CHAKRAVORTY\*

*Department of Physics, and \*Advanced Centre for Materials Science, Indian Institute of Technology, Kanpur, 208 016, India*

Mössbauer, EPR and magnetization experiments have been carried out on the glass composition  $\text{Na}_2\text{O}-\text{SiO}_2-\text{Fe}_2\text{O}_3-\text{Y}_2\text{O}_3$  in which yttrium iron garnet (YIG) can be precipitated by suitable heat-treatment. The measurements have been carried out on the as-quenched sample as well as samples heat-treated for 4 h at 400, 500, 600, 650, 700, 750, 810 and 850° C. Mössbauer spectra from the as-quenched sample as well as the first six samples showed a quadrupole splitting while the last two samples, as well as the sample heat-treated (i) by a two-stage process at 600° C and then at 750° C for 4 h each, and (ii) at 700° C for 40 h, showed a hyperfine as well as quadrupole splitting. The behaviour of the isomer shift (IS) and quadrupole splitting ( $\Delta E$ ) with the heat-treatment temperature show significant changes at the glass transition and crystallization temperatures. The Mössbauer data have been found consistent with optical and electron micrographs which show a large variation in particle size of the precipitated magnetic phase. This has been further correlated with EPR and magnetization data.

## 1. Introduction

Glass ceramics are an important group of materials because of their superior mechanical, thermal and abrasion-resistant properties [1]. Recently, considerable interest has grown in the development of glass ceramics containing magnetic phases, for example lithium ferrite, barium hexa-ferrite, nickel ferrite and manganese ferrite [2-6]. A glass composition  $\text{Na}_2\text{O}-\text{SiO}_2-\text{Fe}_2\text{O}_3-\text{Y}_2\text{O}_3$  in which yttrium iron garnet (YIG) can be precipitated by a suitable heat-treatment has recently been developed in this laboratory [7]. Two techniques, Mössbauer spectroscopy and electron paramagnetic resonance (EPR) have been widely used to study a variety of oxide systems both in crystalline and non-crystalline forms [8-11]. We have carried out such measurements on our glass systems with a view to characterizing the magnetic phases precipitated in the samples after different heat-treatments and the results are reported in this paper.

## 2. Experimental procedure

### 2.1. Sample preparation

The glass composition  $50\text{SiO}_2-34\text{Na}_2\text{O}-10\text{Fe}_2\text{O}_3-6\text{Y}_2\text{O}_3$  (in mol %) was used in the present studies. The glass was prepared from reagent grade chemicals by melting the mixture in an alumina crucible at 1350° C in an electrically heated furnace. Glass plates were cast by pouring the melt onto an aluminium mould. The glass transition temperature ( $T_g$ ) and crystallization temperature ( $T_c$ ) were estimated from DTA analysis using a MOM Hungary, Derivatograph [12]. The samples were then heat-treated at various temperatures.

X-ray powder diffraction patterns for glass-ceramic samples were recorded in a Rich and Seifert ISO-Debyeflex 2002 diffractometer with a  $\text{CrK}\alpha$  target.

### 2.2. Mössbauer measurements

Mössbauer spectra were recorded at room temperature (RT) with a constant acceleration (linear

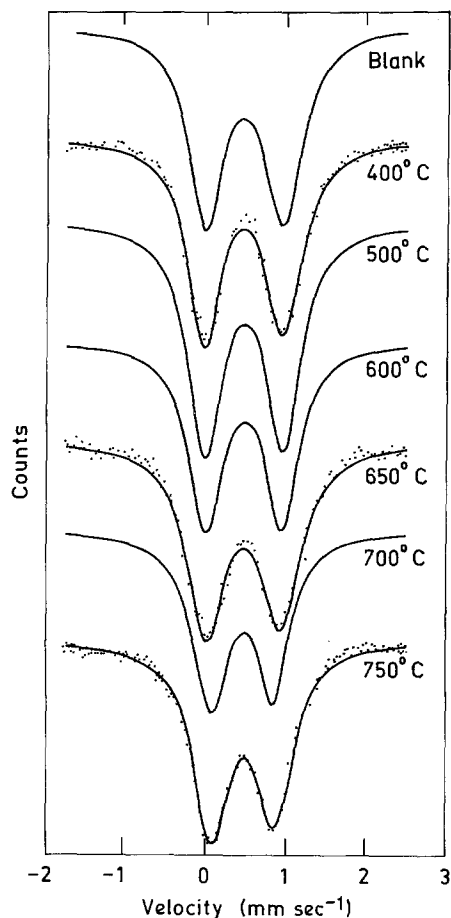


Figure 1 Room-temperature Mössbauer spectra of glass samples heat-treated at different temperatures. The zero of the velocity scale refers to the centroid of the doublet spectrum from sodium nitroprusside.

mode) Mössbauer spectrometer coupled to a multi-channel analyser. The source used was radioactive  $^{57}\text{Co}$  in Rh matrix obtained from New England Nuclear Inc. USA. The spectrometer was calibrated by using the enriched  $^{57}\text{Fe}$  absorber. The glass samples were powdered and approximately 50 mg of the powder was spread uniformly between two layers of sellotape. A least-squares curve-fitting computer program was used to determine the Mössbauer parameters. Standard errors in these parameters were calculated by the usual methods [13].

### 2.3. Other measurements

The EPR measurements were carried out in a Varian Associates Spectrometer (Model V 4502-12) in the X-band frequency and with a 100 kHz field modulation. All the measurements were done at room temperature (RT). Magnetization measure-

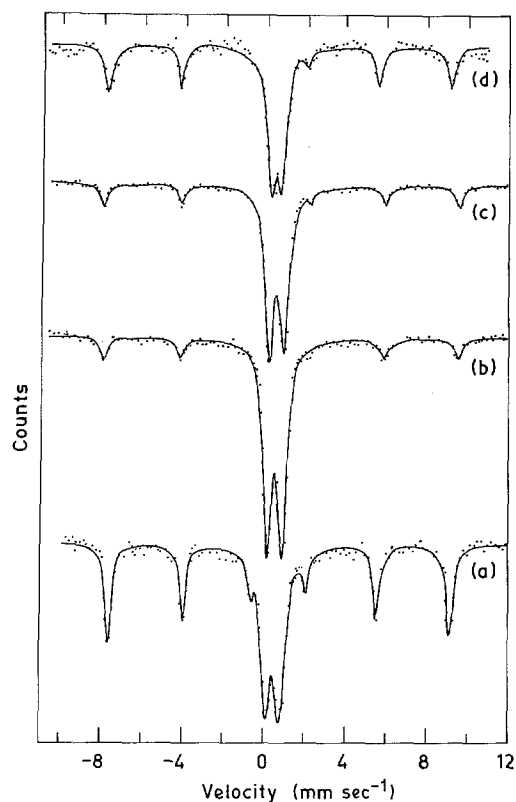


Figure 2 Room temperature Mössbauer spectra of samples heat-treated at (a) 700° C for 40 h, (b) 810° C for 4 h, (c) 850° C for 4 h, and (d) 600 and 750° C for 4 h each. The zero of the velocity scale refers to the centroid of the doublet spectrum from sodium nitroprusside.

ments were performed with a PAR vibrating sample magnetometer (Model 150 A) at room temperature and up to a field of 8 kG.

The transmission electron micrographs of samples heat-treated at different temperatures were taken on a Phillips EM 301 electron microscope. The details of sample preparation will be described elsewhere [14].

### 3. Results and discussion

Mössbauer spectra observed at RT for samples heat-treated for 4 h at different temperatures up to 750° C are shown in Fig. 1. All these spectra show quadrupole splitting only. Mössbauer spectra of some samples heat-treated at (a) 700° C (40 h), (b) 810° C (4 h), (c) 850° C (4 h), and (d) a sample heat-treated at 600° C and 750° C for 4 h at each temperature, show hyperfine splitting as well as quadrupole splitting as seen from Fig. 2. The values of isomer shift (IS) with respect to sodium nitroprusside as determined for the spectra from the quadrupole splitting are plotted against the

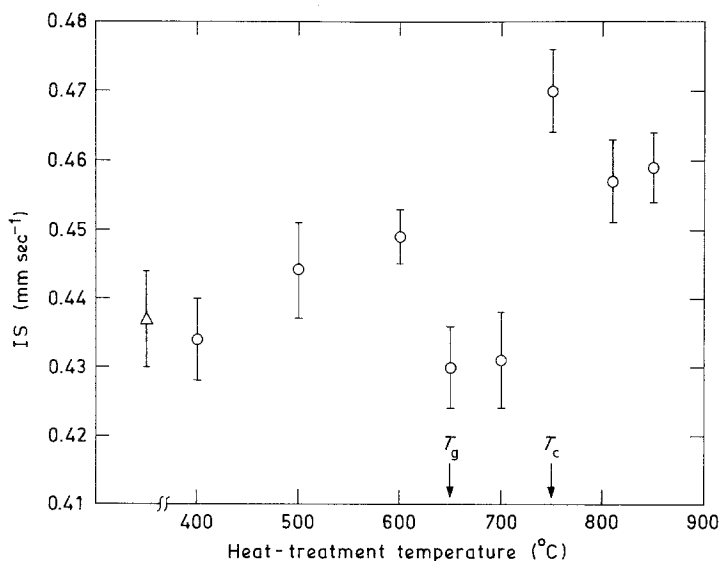


Figure 3 Plot of the isomer shift (IS) determined for the spectra showing quadrupole splitting against heat-treatment temperature. The IS values are given with respect to sodium nitroprusside. Point marked as  $\Delta$  refers to the blank sample.

heat-treatment temperature in Fig. 3 where the glass transition temperature ( $T_g$ ) and the crystallization temperature ( $T_c$ ) for the present glass, determined earlier [7] as  $T_g = 650^\circ\text{C}$  and  $T_c = 750^\circ\text{C}$ , respectively, are also shown. The IS values for all these samples are characteristic of  $\text{Fe}^{3+}$  ion [11, 15]. The value of IS does not change much up to the heat-treatment temperature of  $600^\circ\text{C}$ . However, it shows sharp changes near  $T_g$  ( $650^\circ\text{C}$ ) and  $T_c$  ( $750^\circ\text{C}$ ). The sharp decrease of the IS for the sample heated at  $650^\circ\text{C}$  could be due to incipient phase separation occurring at  $T_g$  prior to nucleation of the crystalline phase. Such a phase separation might give rise to  $\text{Fe}^{3+}$  ions in distorted tetrahedra resulting in a reduction of the IS value. There is a sharp rise in the IS value as the heat-treatment temperature is increased to  $750^\circ\text{C}$  ( $T_c$ ) and it remains high for samples heated at  $810^\circ\text{C}$  and  $850^\circ\text{C}$ , respectively. The IS values for the latter samples as shown in Fig. 3 are determined from the quadrupole splittings. The increase in IS at  $T_c$  and beyond could probably be due to generation of some octahedral  $\text{Fe}^{3+}$  ions which should be present in the garnet phase [11, 16]. The sharp changes in IS at  $T_g$  and  $T_c$  also indicate that the nature of  $\text{Fe}^{3+}\text{-O}^{2-}$  bond changes at these temperatures [3]. The 4s electron density at the tetrahedral site is greater than at the octahedral site in various solids. The Fe—O distance for the tetrahedral site is about 5% smaller than that of the octahedral site. It has been suggested by Van Loef [17] that this difference gives rise to different charge density which could explain the

difference in the IS value at the tetrahedral and octahedral sites of iron in ferrites and garnets.

The value of IS observed for as-quenched (blank) glass was  $0.437 \pm 0.007 \text{ mm sec}^{-1}$  with respect to sodium nitroprusside. This value indicates that  $\text{Fe}^{3+}$  ions are mostly in tetrahedral coordination with a small fraction possibly being in octahedral co-ordination. It is surprising to observe that the samples heated up to  $750^\circ\text{C}$  (4 h) give a quadrupole splitting only. The Mössbauer spectra for the samples in Fig. 1 were also measured at the liquid nitrogen temperature (LNT) although they are not shown here. We did not observe any hyperfine structure for these samples even at LNT. However, the heat-treated samples at  $810^\circ\text{C}$  and  $850^\circ\text{C}$  showed a hyperfine splitting (in addition to the quadrupole splitting) characterized by IS values of  $0.71 \pm 0.05$  and  $0.65 \pm 0.03 \text{ mm sec}^{-1}$ , respectively (Table I). The absence of the hyperfine splittings for the samples heated for 4 h at  $650$ ,  $700$  and  $750^\circ\text{C}$ , indicates that the volume fraction of crystallized YIG phase (which is magnetic) is very small in them. Owing to the small volume fraction of YIG phase, the corresponding hyperfine field probably gets smeared out and the Mössbauer spectra, therefore, show only quadrupole splitting.

As pointed out earlier the Mössbauer spectra in Fig. 2 consist of hyperfine splitting as well as quadrupole splitting. The corresponding Mössbauer parameters are summarized in Table I. The IS values determined for the hyperfine splitting are intermediate between those for octahedral and

TABLE I Mössbauer parameters for samples showing hyperfine as well as quadrupole splitting

Heat-treatment temperature (°C)	Period of heat-treatment (h)	Hyperfine splitting		Quadrupole splitting		Ratio of areas under the hyperfine and quadrupole split peaks
		IS* (mm sec <sup>-1</sup> )	$H_{\text{int}}$ (kOe)	IS* (mm sec <sup>-1</sup> )	$\Delta E$ (mm sec <sup>-1</sup> )	
700	40	0.67 ± 0.03	496 ± 3	0.443 ± 0.017	0.660 ± 0.017	0.96
810	4	0.71 ± 0.05	527 ± 9	0.457 ± 0.006	0.687 ± 0.006	0.16
850	4	0.65 ± 0.03	526 ± 5	0.459 ± 0.005	0.699 ± 0.005	0.22
Two-stage						
(i) 600	4	0.59 ± 0.04	494 ± 4	0.460 ± 0.022	0.519 ± 0.022	0.52
(ii) 750						

\*Values with respect to sodium nitroprusside.

tetrahedral iron while the IS value for the doublet structure indicates the presence of tetrahedral iron predominantly. It is possible that some other phase (such as  $\alpha\text{-Fe}_2\text{O}_3$ ) is also precipitated [16, 18]. This is indicated by the X-ray data also [7]. The amount of this phase could probably be much larger than that of the YIG phase. Another possibility is that the precipitated YIG phase consists of distorted octahedra and tetrahedra giving rise to the observed behaviour (Table I).

A comparison of the Mössbauer spectra of samples heated at 700°C for 4 h and 40 h, respectively, reveals that the former show only quadrupole splitting whereas the latter show quadrupole as well as hyperfine splitting. The hyperfine field ( $H_{\text{eff}}$ ) of the latter measured by us at LNT is greater than that observed at RT. The ratio of the peak-area for the hyperfine splitting to that for quadrupole splitting changes from LNT to RT for the sample heated at 700°C. In addition, this ratio increases as the heat-treatment temperature or the treatment time (at a given temperature) increases (Table I). The magnetization data do not show any saturation behaviour up to a field of 8 kG. All these observations suggest a superparamagnetic behaviour. A systematic examination of

these aspects is planned for future work of the present glass system in our laboratory.

The value of the quadrupole splitting ( $\Delta E$ ) observed for the blank glass is  $0.912 \pm 0.007$  mm sec<sup>-1</sup>. In the case of high spin Fe<sup>3+</sup> ion (3d<sup>5</sup>, 6s<sub>5/2</sub>) the electron distribution is spherically symmetric and therefore should not give rise to any quadrupole splitting. Thus if the normal tetrahedral or octahedral co-ordination is undistorted, no quadrupole splitting should be observed. Kurkjian and Sigety [19] have indicated that there is a large number of non-identical sites with a substantial departure from cubic symmetry in glasses as compared to the situation existing in crystals. This will explain the large quadrupole splitting observed in our glass system. Fig. 4 shows a plot of the quadrupole splitting ( $\Delta E$ ) against heat-treatment temperature of the samples. The  $\Delta E$  value remains essentially constant up to 600°C after which it decreases. It attains a constant value beyond 750°C. These results indicate that the symmetry does not change up to 600°C. At  $T_g$  (650°C) and above, however, due to the nucleation and growth of the crystalline phase the ion sites acquire higher symmetry and as a result the  $\Delta E$  value decreases, ultimately attaining a constant value.

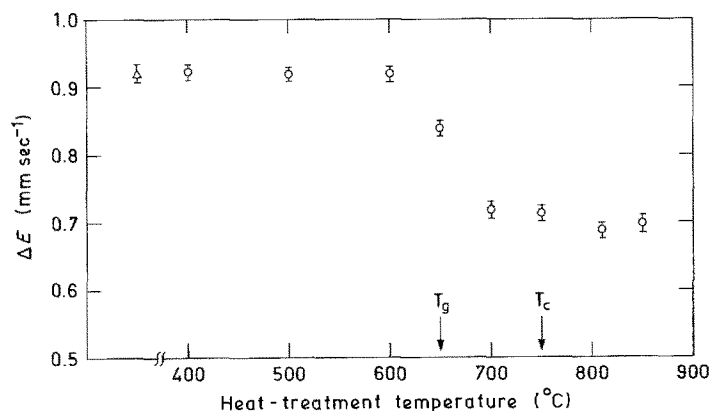


Figure 4 Plot of the quadrupole splitting ( $\Delta E$ ) against the heat-treatment temperature. Point marked as  $\Delta$  refers to the blank sample.

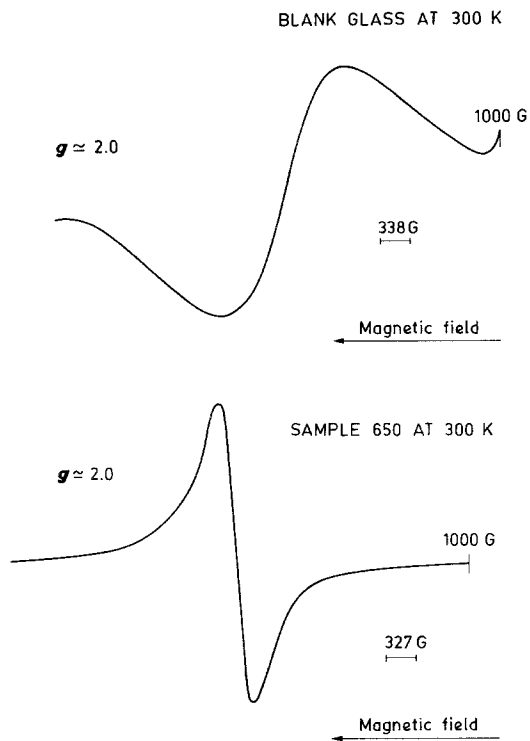


Figure 5 Typical EPR spectra of blank and 650 glass taken at room temperature.

In order to obtain further insight into the coordination and symmetry of iron as well as relaxation phenomenon we carried out EPR measurements on some of our samples and some typical EPR spectra observed at RT are shown in Fig. 5. The corresponding results for the value of  $g$  and the linewidths are given in Table II. The spectra for all the samples show only one resonance which corresponds to a value of  $g$  around 2.0.

The  $g = 4.3$  resonance which usually occurs for paramagnetic  $\text{Fe}^{3+}$  ions [9] is absent in all the samples. This indicates the presence of some type of super-exchange interaction in all the samples (including the blank sample) which exhibit phase separation. A typical micrograph is shown in Fig. 6. It is therefore possible that there is a super-exchange interaction between the iron ions present in the iron-rich phases of these samples. The linewidths for the blank and the sample heat-

TABLE II EPR results

Sample	$g$	$\Delta H$ (G)
Blank	$1.98 \pm 0.02$	$1283 \pm 100$
Heat-treated at $400^\circ\text{C}$	$1.96 \pm 0.02$	$1169 \pm 100$
Heat-treated at $650^\circ\text{C}$	$2.02 \pm 0.02$	$277 \pm 20$
Heat-treated at $750^\circ\text{C}$	$1.94 \pm 0.02$	$268 \pm 20$

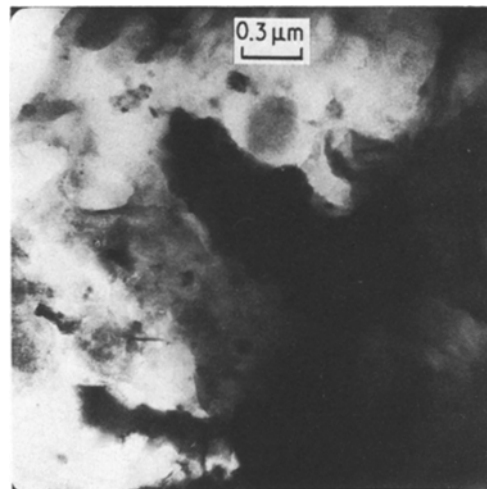


Figure 6 A typical electron micrograph of the blank glass.

treated at  $400^\circ\text{C}$  are nearly identical. However, there is a sharp decrease in the linewidth for the samples heat-treated at  $650$  and  $750^\circ\text{C}$ . A similar observation has also been made in the variation of  $\Delta E$ . The value of  $g$  of the sample heat-treated at  $650^\circ\text{C}$  is in agreement with that of YIG [20]. The decrease in the linewidth as a function of heat-treatment temperature is apparently caused by an increase in the super-exchange interaction following the precipitation of the magnetic phase within the glass. A typical electron and optical micrograph of the sample heated at  $650^\circ\text{C}$  is shown in Fig. 7 to illustrate the wide range of particle size present in the system. Similar behaviour has been observed for other samples heated above  $650^\circ\text{C}$  with a general trend of the growth of particle size with heat-treatment temperature. Such behaviour has also been observed in the case of thin films of garnets heat-treated at various temperatures [21]. The wide range of particle size observed by us can be the cause behind the simultaneous occurrence of hyperfine structure and quadrupole splitting for samples referred to in Table II.

The variation of magnetic susceptibility with temperature is shown in Fig. 8. A sharp rise in the curve observed at  $650^\circ\text{C}$  is attributed to the precipitation of the magnetic phase. A similar result has been reported in the case of basalt glass ceramics [9].

Further studies of the present glass system are in progress with the aim of delineating the influence of phase separation on the kinetics of crystallization.

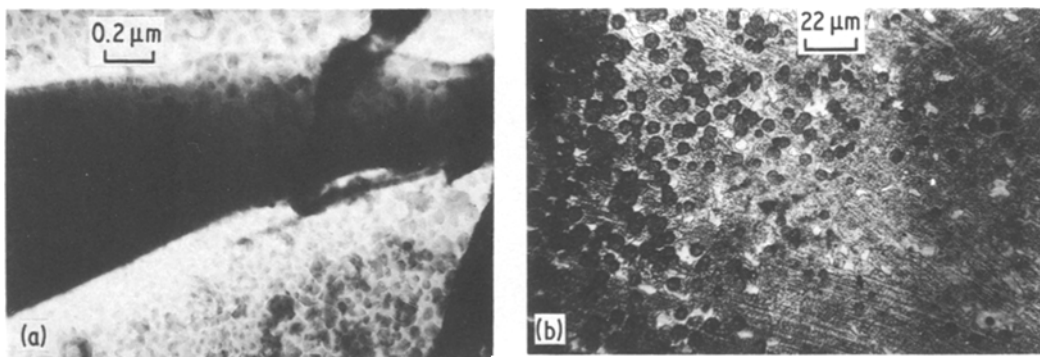


Figure 7 Typical (a) electron, and (b) optical micrographs of the 650 sample.

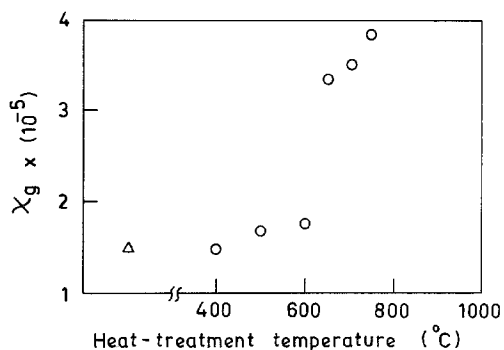


Figure 8 Plot of the magnetic susceptibility against heat-treatment temperature, treatment time 4 h.

### Acknowledgements

The authors wish to thank Mr N. V. Nair for his help in the Mössbauer measurements. The investigation was supported partly by a grant received from the Department of Science and Technology, Government of India.

### References

- P. W. McMILLAN, "Glass Ceramics" (Academic Press, New York, 1979).
- T. KOMATSU, N. SOGA and M. KUNUGI, *J. Appl. Phys.* **50** (1979) 6469.
- T. KOMATSU and N. SOGA, *ibid.* **51** (1980) 601.
- R. R. SHAW and J. H. HEASLEY, *J. Amer. Ceram. Soc.* **50** (1967) 297.
- W. J. S. BLACKBURN and B. P. TILLEY, *J. Mater. Sci.* **9** (1974) 1265.
- B. T. SHIRK and W. R. BUESSEM, *J. Amer. Ceram. Soc.* **53** (1970) 192.
- D. BAHADUR, B. SHARMA and D. CHAKRAVORTY, *J. Mater. Sci. Lett.* **1** (1982).
- T. RAMAN, G. N. RAO and D. CHAKRAVORTY, *J. Non-Cryst. Solids* **29** (1978) 85.
- A. K. BANDOPADHYA, J. ZARZYCKI, P. AURIE and J. CHAPPERT, *ibid.* **40** (1980) 353.
- V. G. JADHAO, R. M. SINGRU, G. N. RAO, D. BAHADUR and C. N. R. RAO, *J. Chem. Soc. Faraday Trans. II* **71** (1975) 1885.
- C. R. KURKJIAN and E. A. SIGETY, *Phys. Chem. Glass* **9** (1968) 73.
- G. C. DAS, T. K. REDDY and D. CHAKRAVORTY, *J. Mater. Sci.* **13** (1978) 3211.
- V. J. LAW and R. W. BAILEY, *Chem. Eng. Sci.* **18** (1963) 189.
- P. SARKAR, J. KUMAR and D. CHAKRAVORTY, *J. Mater. Sci.* (to be published).
- J. DANNON, in "Chemical Applications of Mössbauer Spectroscopy", edited by V. I. Goldanskii and R. H. Herber (Academic Press, New York, 1968) p. 159.
- K. J. KIM, M. P. MALEY and R. K. MACRONE, in "Amorphous Magnetism", Vol. II, edited by R. A. Levy and R. Hasegawa (Plenum Press, New York, 1977) p. 627.
- J. J. VAN LOEF, *Physica* **32** (1966) 2102.
- W. KÜNDIG, H. BOMMEL, G. CONSTABAVIS and R. H. LINDQUIST, *Phys. Rev.* **142** (1966) 327.
- C. R. KURKJIAN and E. A. SIGETY, *Phys. Chem. Glasses* **5** (1964) 63.
- W. H. VON AULOCK, "Handbook of Microwave Ferrite Materials" (Academic Press, New York, 1965).
- D. BAHADUR and K. N. RAI, *Mater. Res. Bull.* **15** (1980) 501.

Received 4 December 1981  
and accepted 11 February 1982